

基于薄板搭接的互感式焊缝跟踪传感器的分析

洪 波, 刘 湘, 何荣拓, 阳佳旺

(湘潭大学 机械工程学院, 湘潭 411105)

摘 要: 采用双矩形截面圆柱线圈互感式传感器作为焊缝跟踪传感器, 实现了薄板搭接的焊缝跟踪. 利用等效圆形回路法计算了轴线相交的矩形截面圆柱线圈之间的互感系数. 使用 Ansys 有限元分析软件, 建立了传感器的三维模型, 对传感器线圈的参数进行了优化设计, 分析了线圈轴线夹角对于传感器输出的影响, 确定了适合于焊缝跟踪的互感式传感器结构. 最后进行了互感式焊缝跟踪传感器的焊缝跟踪具体试验, 传感器输出线性度良好, 跟踪精度达到要求, 为薄板搭接的自动焊缝跟踪技术提供了新的方法.

关键词: 薄板搭接; 互感式; 有限元分析; 焊缝跟踪

中图分类号: TG 409 **文献标识码:** A **文章编号:** 0253-360X(2014)09-0015-04

0 序 言

发展和应用新型焊缝自动跟踪技术是提高焊接自动化水平的必然要求. 焊缝跟踪就是在焊接时检测出焊缝的偏差, 并调整焊接路径和焊接参数, 保证焊接质量的可靠性. 因此根据具体的焊接种类以及周围环境选用合适的传感器来检测焊缝偏差信息尤为重要^[1-2]. 由于传统的机械接触式传感器有适用的坡口形式少、探头磨损大等缺点, 所以其应用受到限制. 虽然目前电弧传感器得到广泛应用, 但其应用在搭接接头、不开坡口的对接接头等形式时, 仍不能准确识别^[3].

薄板搭接焊缝作为工业生产中的一种非常广泛应用的焊接坡口形式, 其焊缝的自动跟踪一直得不到良好的解决方案^[4]. 文中针对薄板搭接焊缝, 设计了一种双线圈互感式的焊缝跟踪传感器, 成功应用于薄板搭接焊缝的跟踪, 且跟踪效果良好, 为焊缝跟踪技术提供了新的方法.

1 互感式焊缝跟踪传感器原理

互感式焊缝跟踪传感器的工作原理是通过两个矩形截面圆柱线圈呈一定的角度置于焊缝坡口的上方, 其中激励线圈 L_1 通过由振荡器产生的高频电压

信号 U_1 线圈中即流过一个同频率的交流电流, 并在其周围产生一个交变磁场. 于是感应线圈 L_2 的两端会产生一交变电动势 U_2 .

图1所示为互感式传感器与工件的位姿关系. 互感式传感器的双线圈探头通过支架与焊枪固定在一起并前置与焊枪. 当焊接进行时, 传感器探头提前探测焊枪与坡口的对中情况. 当传感器左偏的时候, 由于传感器线圈呈夹角, 空气的磁导率很低, 所以由激励线圈 L_1 发出的磁力线经空气传导只有很

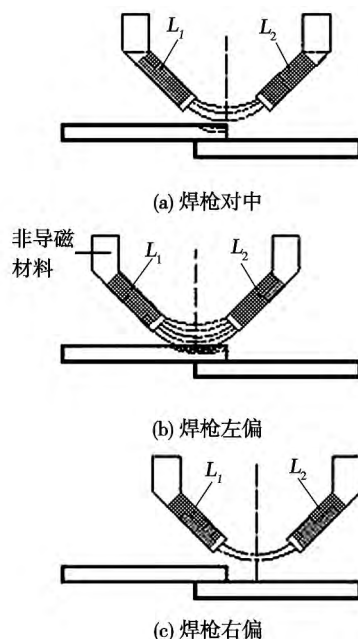


图1 互感式传感器焊缝跟踪原理

Fig. 1 Principle of mutual inductance seam tracking sensors

收稿日期: 2013-03-20

基金项目: 国家自然科学基金资助项目(50975243); 湖南省战略性新兴产业产学研结合创新平台创新能力资助项目(2012GK4100); 湖南省科技计划重点资助项目(2012XK4068)

少一部分能到达感应线圈,但是由于焊接工件会产生涡流效应,集中于表面,使得磁力线返回或者到达感应线圈,因此感应线圈端的感应电动势 U_2 明显增大. 电动势 U_2 明显增大. 反之传感器右偏时,由于激励线圈与感应线圈磁回路中空气磁导占主要部分,则感应电动势相对于传感器对中时明显减小. 感应电动势经后续的信号放大与转换电路,通过一定的延迟处理,经由单片机对比输出以控制信号给十字滑块上的步进电机来调整焊炬的位置,进行偏差纠正,从而保证了薄板搭接的焊缝自动跟踪.

2 非共轴互感式传感器的电感计算

2.1 等效圆环回路法

互感式焊缝跟踪传感器是利用激励线圈在接收线圈中产生的感应电动势的变化来提取焊缝的位置信息. 感应电动势的大小,根据电磁感应定律可得

$$E_{L_2} = \frac{\Delta \psi_{21}}{\Delta t} \quad (1)$$

式中: ψ_{21} 为磁通量; Δt 为变化时间.

设两线圈的互感系数为 M ,将式(1)代入得

$$E_{L_2} = \frac{\Delta(M i_1)}{\Delta t} = M \frac{\Delta i_1}{\Delta t} \quad (2)$$

式中: i_1 为线圈的电流; Δi_1 为线圈的变化电流. 因此确定两线圈的互感系数则可以得出感应线圈的感应电动势.

由于传感器的矩形截面线圈非共轴,因此为了计算其线圈间的互感,引入等效圆形回路法来简化模型. 这种方法的实质可归结为将每个线圈用两个“等效圆环电路”即轴向等效回路和径向等效回路来代替^[5,6],确定圆环的直径和位置后,在相应的磁势之下(对应的电流和匝数)两个回路产生的磁场近似的等于原线圈产生的磁场,如图2所示.

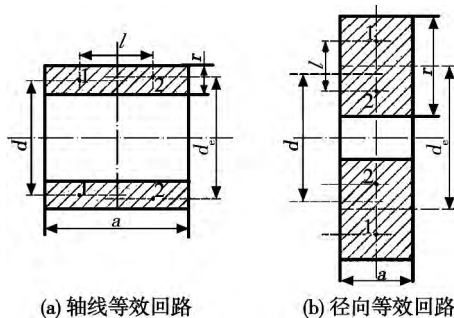


图2 等效圆形回路示意图

Fig. 2 Schematic diagram for equivalent circular loop

所求互感可用下式确定,即

$$M = \frac{N_1 N_2}{4} (M_{13} + M_{14} + M_{23} + M_{24}) \quad (3)$$

式中: N_1 为激励线圈匝数; N_2 为感应线圈匝数; M_{13} 为圆形回路(轴线)1和3的互感; M_{14} 为圆形回路1和4的互感; M_{23} 为圆形回路2和3的互感; M_{24} 为圆形回路2和4的互感.

等效回路与原线圈同轴,对于线圈轴线尺寸 a (长度)大于它的径向尺寸 r (线圈厚度),则它对应的回路直径为

$$d_e = d \left(1 + \frac{r^2}{6d^2} \right) \quad (4)$$

式中: $d = (r_1 + r_2) / 2$; r_1 为线圈内圈半径; r_2 为线圈外圈半径.

两回路关于线圈轴对称,彼此间的距离为

$$b = \sqrt{|a^2 - r^2|} / 3 \quad (5)$$

如果 $a < r$,则回路处于线圈的对称平面上,回路的直径为式(4)中的 $d_e + l$ 和 $d_e - l$. 而对于正方形截面线圈 $r = a$, $b = 0$,即两个回路合并为一个,更加简化计算.

2.2 轴线相交的两个线圈之间的互感系数的确定

根据等效圆环回路法,由于线圈长度远大于线圈厚度,因此将用于焊缝跟踪的互感式传感器等效为轴线相交的4个圆形回路来分析^[7,8],如图3所示. 建立坐标系,左右两个线圈关于 y 轴对称,线圈与 y 轴之间的夹角为 θ ,假设两线圈匝数、几何参数均一样,线圈长度为 a ,4个圆环回路的圆心坐标分别为 (x_1, y_1) , (x_2, y_2) , (x_3, y_3) 和 (x_4, y_4) .

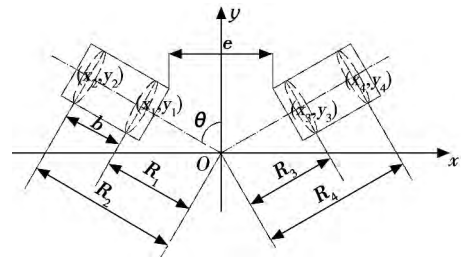


图3 互感式焊缝跟踪传感器等效示意图

Fig. 3 Equivalent schematic diagram for mutual inductance seam tracking sensors

根据等效圆形回路法,得出图3中各参数为

$$\left. \begin{aligned} R_1 &= R_3 = \frac{a-b}{2 \sin \theta} + \frac{e}{2} \\ R_2 &= R_4 = \frac{a-b}{2 \sin \theta} + \frac{e}{2} + b \end{aligned} \right\} \quad (6)$$

式中: e 为两线圈末端距离.

根据式(3)可知,只需求出两两圆环回路之间的互感,即可得出两线圈之间的互感,把轴线相夹的

两圆形回路简化为一次数值积分计算,即

$$M_{13} = \frac{\mu b}{4\pi^2} \int_0^\pi \frac{fF}{A^{3/2}} d\theta \quad (7)$$

式中: μ 为相对磁导率; F 为常数; f 和 A 是由 θ 决定的参数; θ 为线圈与 y 轴之间的夹角。

$$A^2 = 1 - \sin^2 \frac{\theta}{2} \cos^2 \theta - \frac{2c}{b} \cos \frac{\theta}{2} \cos \theta + \left(\frac{c}{b} \right)^2 \quad (8)$$

$$f = \cos \frac{\theta}{2} - \frac{c}{b} \cos \theta, \quad c = b \sin(\theta/2) \quad (9)$$

同理,可得 M_{14} 、 M_{23} 、 M_{24} 。

综合式(1)~式(9)可得出互感系数为

$$E_{L_2} = f(\mu, N, a, r, \theta) \quad (10)$$

式中: N 为线圈匝数,如果保持 a 、 N 、 r 和 θ 等参数不变,根据式(10)可知,介质的相对磁导率 μ 则为感应线圈电动势的单值函数,当双线圈互感式传感器偏移焊缝中心时,由于钢板中涡流趋肤效应的存在,使得传感器周围相对磁导率也发生明显变化,因而线圈 L_2 的感应电动势的输出大小也随之发生明显变化,从而可以判断焊炬的左右偏移。

3 互感式传感器的有限元分析

3.1 传感器线圈的 Ansys 建模

根据互感式焊缝跟踪传感器的原理,考虑传感器本身参数、位置和搭接工件钢板等因素,运用节点三维谐波法对互感式焊缝跟踪传感器进行有限元分析。建立了如图4所示的 Ansys 3D 分析模型。

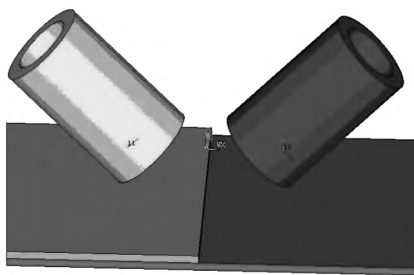


图4 互感式焊缝跟踪传感器 Ansys 3D 分析模型

Fig. 4 Ansys 3D analysis model of mutual inductance seam tracking sensors

3.2 互感式焊缝跟踪传感器线圈的参数优化

式(10)中已经得出与传感器感应线圈的感应电动势有直接关联的一些参数,首先根据 Ansys 强大的参数优化功能,对线圈自身的参数进行优化设计,以获取感应线圈电动势最大为目标函数,对传感器两线圈自身参数做多次 Ansys 分析。首先固定输入

频率为 600 kHz 输入电流 6 A,从线圈匝数 N 开始,对线圈长度 a 、线圈厚度 r 、线圈末端距离 e 和线圈与 y 轴之间的夹角 θ 逐个进行参数优化,优化之后的最适合参数作为下一个参数优化的输入定值。结果如表1、表2和图5所示。

表1 线圈匝数的参数优化

Table 1 Parameter optimization for the turns of coil

线圈匝数 N	感应电动势 E_{L_2} /mV
400	0.718
500	0.996
600	1.180
700	1.590

表2 线圈长度的参数优化

Table 2 Parameter optimization for the length of coil

线圈长度 a /mm	感应电动势 E_{L_2} /mV
15	0.047
20	1.590
25	0.140
30	0.195

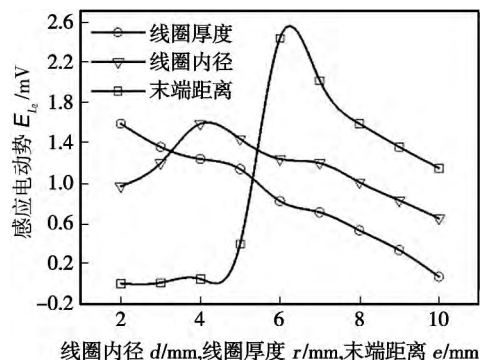


图5 线圈参数优化结果

Fig. 5 Figure for parameter optimization results of coil

经过 Ansys 有限元分析,对传感器线圈的每个参数进行了参数优化,得出当线圈厚度为 2 mm、线圈内径为 4 mm、线圈末端距离为 6 mm 时,互感式传感器两线圈感应输出电动势最大。有利于进行对传感器输出信号的采集与处理,从而提高了焊缝跟踪的精度。

3.3 线圈两轴夹角对于传感器输出的影响

固定传感器自身线圈参数不变,分析传感器线圈两轴之间的夹角 (2θ) 对于传感器输出的影响规律。选取夹角为 $60^\circ \sim 120^\circ$ 变化时,进行 Ansys 有限元仿真分析,得出结果如图6所示。

当线圈自身参数一定,两线圈轴间夹角为 90° 时,传感器感应线圈输出感应电动势最大。

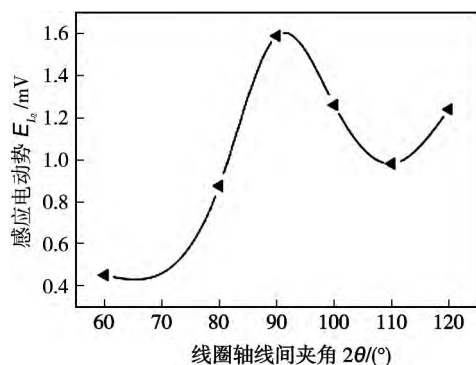


图 6 线圈轴线夹角对于传感器输出的影响

Fig. 6 Impact on the sensor output by the change of coil axis angle

4 传感器的跟踪特性分析

根据前面章节 Ansys 对于互感式焊缝跟踪传感器的结构设计及输出影响因素分析,根据线圈参数优化结果,绕制了两矩形截面圆柱线圈。

通过波形发生器输入 600 kHz 的振荡交流电压,通过功率放大电路作为激励源输入至传感器激励线圈,输出的感应电动势则通过数字示波器查看。分析输入/输出波形,得出传感器的响应时间在 9 ~ 11 ms 之间,表明传感器的响应及时性良好。

传感器本身与焊枪固定在一起前置与焊炬 1 cm,试验时传感器线圈整体与焊接搭接工件钢板的距离为 4 mm,薄板厚 1 mm。通过不断调整焊枪的位置,查看数字示波器输出的感应电动势变化,具体试验数据如图 7 所示。当焊枪左右偏离时,传感器感应线圈输出值线性变化良好,有利于焊缝跟踪信号的提取。

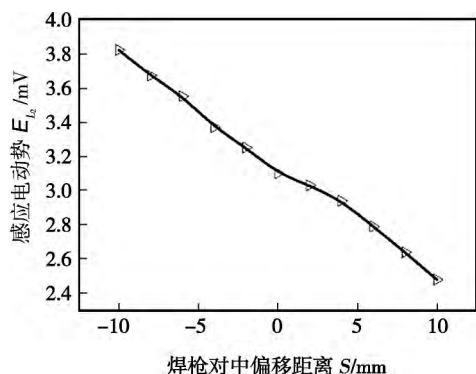


图 7 互感式焊缝跟踪传感器输出特性曲线

Fig. 7 Output characteristic curve of mutual inductance seam tracking sensors

5 结 论

(1) 针对薄板搭接焊缝,设计了一种互感式焊缝跟踪传感器,采用等效圆环回路法得出互感式传感器两线圈之间的互感系数。

(2) 当输入电流大小和频率一定时,由 Ansys 有限元分析可得出互感式传感器的输出电动势大小分别与传感器线圈匝数、长度、厚度、末端距离、线圈与 y 轴之间的夹角间的变化关系,为优化互感式传感器参数提供了理论参考。

(3) 通过互感式焊缝跟踪传感器跟踪特性试验表明,传感器感应线圈输出特性曲线线性度良好。输出值线性变化明显,有利于焊缝跟踪信号的提取。

参考文献:

- [1] 周 律,陈善本,林 涛. 弧焊机器人焊缝跟踪方法的研究现状[C]// 第十一次全国焊接会议,上海,2005,33-35.
- [2] 潘际奎. 现代弧焊控制[M]. 北京:机械工业出版社,2000.
- [3] 洪 波,魏复理,来 鑫,等. 一种用于焊缝跟踪的磁控电弧传感器[J]. 焊接学报,2008,29(5):1-4.
Hong Bo, Wei Fuli, Lai Xin, et al. A magnetic control arc sensor for seam-tracking[J]. Transactions of the China Welding Institution, 2008, 29(5): 1-4.
- [4] 洪宇翔,向小明,洪 波,等. 一种应用于薄板搭接的磁控电弧焊缝跟踪方法[J]. 焊接学报,2013,34(10):67-70.
Hong Yuxiang, Xiang Xiaoming, Hong bo, et al. A seam tracking method for overlap sheet welding based on magnetic-control arc sensing[J]. Transactions of the China Welding Institution, 2013, 34(10): 67-70.
- [5] 卡兰塔罗夫 II II,采伊特林 II A. 电感计算手册[M]. 陈汤铭,译. 北京:机械工业出版社,1992.
- [6] Babic S. Akyel between circular C. calculating mutual inductance coils with inclined axes in air[J]. IEEE Transactions on Magnetics, 2008, 44(7): 1743-1750.
- [7] Pankrac V. Generalization of relations for calculating the mutual inductance of coaxial coils in termstheir applicability to non-coaxial coils[J]. IEEE Transactions on Magnetics, 2011, 47(11): 4552-4563.
- [8] Engel K, Mueller D. High-speed and high-accuracy method of mutual inductance calculations[J]. IEEE Transactions on Plasma Science, 2009, 37(5): 683-692.

作者简介:洪 波,男,1960 年出生,博士,教授。主要从事焊接方法、设备及自动化和仿真建模、数值计算等方面的科研和教学工作。发表论文 50 余篇。Email: hongbo@xtu.edu.cn

MAIN TOPICS ,ABSTRACTS & KEY WORDS

Effect of trace CO₂ on arc-ultrasonic TIG welding of MGH956 alloy LEI Yucheng^{1,2}, LUO Ya¹, REN Dan¹, LI-ANG Shenyong¹ (1. School of Material Science and Engineering , Jiangsu University , Zhenjiang 212013 , China; 2. Jiangsu Province Key Laboratory of High-end Structural Materials , Zhenjiang 212013 , China) . pp 1 - 5

Abstract: Trace CO₂ was added in the shielding gas during MGH956 alloy arc-ultrasonic TIG welding , and the mechanism and influence law of trace CO₂ on the microstructure and properties of the joint were analyzed. The results show that the grains in the weld grew smaller , the porosity in the weld became less , and the tensile strength of the joint increased. Based on the effect of the arc-ultrasonic , after 0.5% CO₂ was added in pure Ar , the grains in the weld center were fine-equiaxed and uniformly distributed in the weld , the tensile strength of the joint enhanced significantly , and the joint fracture mode changed from brittle fracture to ductile fracture. Meanwhile , the hardness of the weld increased after trace CO₂ was added in the shielding gas , and the comprehensive properties of the joint were improved.

Key words: MGH956 alloy; TIG welding; arc-ultrasonic; trace CO₂; microstructure

Characteristics of joint and interface layer during bypass-current MIG welding-brazing of aluminum and steel dissimilar metals MIAO Yugang¹, WU Binta², HAN Duanfeng¹, XU Xiangfang² (1. National Key Laboratory of Science and Technology on Underwater Vehicle , Harbin Engineering University , Harbin 150001 , China; 2. College of Shipbuilding Engineering , Harbin Engineering University , Harbin 150001 , China) . pp 6 - 10

Abstract: By pass-current MIG welding-brazing was conducted with 2 mm thick 6061 aluminum alloy plates and galvanized steel plates. The microstructure and mechanical properties of lap joints were investigated by optical microscopy , scanning electron microscope with energy dispersive spectrometer and tensile testing. The effect of welding speed on interface layer and joint characteristics during by pass-current MIG welding-brazing of aluminum alloy to steel was analyzed. The results show that with the increase of welding speed , the welding heat input reduced , and the interface temperature dropped which decreased the diffusion of elements and finally reduced the thickness of interface layer. In addition , the tensile strength of joint tended to increase at first and then reduce with the increase of welding speed , and reached a maximum of 135.32 MPa. When the welding speed was low , the high interface temperature increased the possibility of forming brittle intermetallic compounds which would reduce the performance of the resultant joint. On the contrary , defects such as incomplete brazing and pores in the interface because of insufficient reaction could occur at higher welding speed.

Key words: bypass-current MIG welding-brazing; dissimilar metals; welding speed; interface

Mechanical behavior of IMC in BGA soldered joints by nanoindentation method WANG Lifeng , Dai Wenqin , ZHANG Pule , MENG Gongge (College of Materials Science and Engineering , Harbin University of Science and Technology , Harbin 150040 , China) . pp 11 - 14

Abstract: Nanoindentation experiments were carried out on (Cu ,Ni)₆Sn₅ , Cu₆Sn₅ and Cu₃Sn IMCs in BGA soldered joints. The influence of loading velocity on the mechanical behavior of intermetallic compounds was investigated. The Young's modulus and nanoindentation hardness of (Cu ,Ni)₆Sn₅ , Cu₆Sn₅ and Cu₃Sn IMCs were obtained from load-depth curves with Oliver-Pharr method. The results indicate that serrated rheological effect was related to the load rate. All of three kinds of IMC , including Cu₆Sn₅ , Cu₃Sn and (Cu ,Ni)₆Sn₅ , showed serrated rheological effect with different degrees when the loading rate was low. However , the serrated rheological effect was not obvious for Cu₃Sn and (Cu ,Ni)₆Sn₅ , except for Cu₆Sn₅ , when the loading rate increased. The Young's modulus of (Cu ,Ni)₆Sn₅ , Cu₆Sn₅ and Cu₃Sn IMCs were 126 GPa , 118 and 135 GPa , respectively. The nanoindentation hardness of (Cu ,Ni)₆Sn₅ , Cu₆Sn₅ and Cu₃Sn IMCs were 6.5 , 6.3 and 5.8 GPa , respectively. The Young's modulus and nanoindentation hardness of (Cu ,Ni)₆Sn₅ were higher than those of Cu₆Sn₅.

Key words: nanoindentation; intermetallic compound; serrated rheological effect; mechanical behavior

Seam tracker of mutual-inductance based on sheet lapping

HONG Bo , LIU Xiang , HE Rongtuo , YANG Jiawang (Department of Mechanical Engineering , Xiangtan University , Xiangtan 411105 , China) . pp 15 - 18

Abstract: Using a double-coiled rectangle cross section of cylinder mutual-inductive sensor as seam-tracking sensor , the tracking of steel sheet lapping was realized. The mutual-inductance coefficient of the axes-intersecting coils was calculated with the cycle loop method. A 3D model was built for the sensor through Ansys software. After optimizing the parameters of the coils and analyzing the influence of the angle between coils on the output of sensor , the structure of mutual-inductive sensor was defined for seam tracking. The experimental results show that the linearity of sensor output was fine and the tracking precision fulfilled the requirements. This research provides a new way for automatic seam-tracking of lapping sheet.

Key words: lapping of steel sheet; mutual-inductive; finite element analysis; seam-tracking

Effect of activating flux on laser arc hybrid welded stainless steel YIN Yan¹, WANG Zhanchong¹, ZHANG Ruihua², YUAN Zhengwei¹, TA Jinguo¹ (1. State Key Laboratory of Gan-